EVALUATION OF ELECTROMAGNETIC DOSIMETRY OF WIRELESS SYSTEMS IN COMPLEX INDOOR SCENARIOS WITH HUMAN BODY INTERACTION

E. Aguirre[1], J. Arpón[1], L. Azpilicueta[1], S. de Miguel[2], V. Ramos[2], and F. Falcone[1, *]

[1]Electrical and Electronic Engineering Department, UPNA, Pamplona, Navarra, Spain

[2]Telemedicine and E-Health Research Unit, Health Institute Carlos III, Madrid, Spain

Abstract—In this work, the influence of human body within the estimation of dosimetric values is analyzed. A simplified human body model, including the dispersive nature of material parameters of internal organs, skin, muscle, bones and other elements has been implemented. Such a model has been included within an indoor scenario in which an in-house 3D ray launching code has been applied to estimate received power levels within the complete scenario. The results enhance previous dosimetric estimations, while giving insight on influence of human body model in power level distribution and enabling to analyze the impact in the complete volume of the scenario.

1. INTRODUCTION

The use of wireless systems has experienced great growth in the last decade, mainly due to the adoption of communication systems that are of use in a broad range of applications. One of the areas experiencing more growth is the adoption of wireless systems in indoor scenarios, with the advent of Wireless Sensor Networks for health monitoring and home automation system of the evolution of mobile wireless systems, with Long Term Evolution being the main driver in femtocell deployment. In the case of a conventional household, several wireless systems can be operating simultaneously, such as WLAN in different versions, personal area network such as Bluetooth or ZigBee, or distribution in wireless fashion of DVB-T

signals, among others. Also, Ambient Assisted Living scenarios make intensive use of wireless sensors in order to perform monitoring and control tasks, adding new elements of use within the wireless spectrum (mainly based on 802.15 standard as well as GSM/UMTS backup). Because of this growth of wireless technology it is highly important to have the knowledge of the effects that exposure to electromagnetic fields has in the human body. Related to this, there are several organizations that are devoted to legislate issues and recommendations in this area, establishing maximum limits to which a person may be exposed [1, 2]. In this scenario, dosimetric assessments acquire great importance due to the fact that they determine whether new legislation should be implemented and anticipating potential changes in actual regulations, with an extensive set of dosimetric assessments reported in literature [3–6], with different techniques and different approaches of the human body more or less accurate or simplified.

A priori, the most precise way to estimate electromagnetic exposure and perform dosimetric evaluation is obtained by in situ measurements. However, to obtain insight on the potential impact of different wireless devices and their integration as complete systems requires the use of theoretical estimations. On the other hand, these theoretical estimations exhibit some problems, related to the accuracy of the radio propagation parameters and to the human body characteristics. This leads to a commitment between the computational complexity in terms of calculation time and the final accuracy of the results.There is a great assortment of ways to estimate radio propagation and a large ways of representing the human body. The most accurate method to perform dosimetric estimation is directly solving Maxwell's equations,in which SAR calculations are achieved using full wave techniques such as Finite Difference Time Domain [7–9], or equivalent methods. However, the large requirements in terms of memory use and the high computational cost make them inappropriate for large area calculations at high frequency bands. The search for optimized evaluation of SAR values has lead to enhanced estimation procedures, including modification of the measurement setup to maintain level of exposure and field uniformity, such as described in [10].

Geometrical optics techniques offer a good approximation with a lower computational cost. This group includes a great number of methods, being one of the most widespread the Shooting and Bouncing Rays (SBR) [11–13]. Another approach is the use of empirical methods, traditionally applied for initial coverage estimation of broadcast wireless systems. They give rapid results but require calibration based on measurements to give an adequate fit of the

results based on initial regression methods (elimination of mean error component and reduction of standard deviation). These methods are not optimal for dosimetry studies due to the complexity of the human body in morphological as well as topological terms, although they have been used to perform initial estimations [14].

The human body model designed for simulations can be more or less complex depending on the required analysis and the frequencies of operation of the wireless systems under consideration.Several studies simplify the human body by representing it cylindrically [15–17], spherically [14, 18–20] or with ellipsoidal shape [21–23]. Generally, the aim of these studies is the analysis of the influence of the total human body in the environment, although there are also studies related to specific body parts [24].

Within the variety of morphologically similar human body models, there are high resolution models [25–27], which show a dense volume meshing; or simpler ones [28–30] that respect the basic structure of the arms, legs, head, etc.. It should be noted that depending of the aim of the analysis or the substantial processing time, many studies that implement a high resolution model focus in a localized area of the body and not in the overall human body [31, 32]. Many of these models are also studied experimentally, with the so-called phantom models, which are designed similarly with a variety of shapes [33, 34].

The goal of this work is to obtain dosimetric assessments in large spaces considering the interaction of the environment and the objects that are located within this scenario and not an isolated human body or a fraction of it. This is achieved by an adequate balance between computational time and accuracy of data, with the best combination of radio propagation estimation technique with simplified model of the human body. Considering all methods described, geometrical optics technique is optimal because although it is not as accurate as full wave techniques, it offers good results, with standard deviations of 5–8 dB [35], with a fairly low computational cost. As far as the simplified model of the human body is concerned, the use of cylindrical model could be interesting, providing good results in high intermediate frequencies (400 MHz to 7 GHz) [36]. Nevertheless, is recommendable a high resolution model, considering the computational time and the complexity of implementation, for more precise analysis.

In the literature, electromagnetic and thermal analysis has been performed in the human head due to RF exposure [37, 38], relating interaction of electromagnetic fields in the calculation of Specific Absorption Rate. Non-thermal effects have also been analyzed, basically on the influence of time and frequency hopping mechanisms in REM sleep stages as well as in alpha waves [39, 40]. In both

cases, the estimation of the received electromagnetic field value is a key parameter in the rf exposure analysis. The aim of this article is to assess in the computation of received electromagnetic field values, which can later on be employed as an estimation of compliance with international, national and local standards. This methodology is actually employed by Spanish Ministry of Health in the verification of regulation compliance, by means of RMS measurement of 1 second samples in a 6 minute time span per measurement location of E-field values. The goal is an analysis of an indoor scenario with the presence of a human body model to verify his influence in the environment. It is shown that the topology and morphology of the scenario strongly influence the behavior of the wireless channel. A deterministic method based on three-dimensional (3D) ray launching has been implemented within our research team based on Matlab^{TM} programming environment. A simplified human body model has been developed for this code. This model implements the basic organs considering their frequency dispersive material characteristics, in order to analyze their influence on the environment. The combination of a simplified human body model with an efficient simulation technique enables to assess the impact of wireless systems within the complete scenario under analysis, not limited to specific body sections.

2. DEFINITION OF SIMULATION SCENARIOS AND RESULTS

Deterministic methods [41–47] are based on numerical approaches to the resolution of Maxwell's equations, such as ray launching and ray tracing, or full-wave simulation techniques (method of moment (MoM), finite difference time domain (FDTD) [48], FITD, etc.). These methods are precise but are time-consuming to inherent computational complexity. As a midpoint, methods based on geometrical optics, offer a reasonable trade-off between precision and required calculation time [49]. As stated in the introduction, a 3D ray launching algorithm has been implemented in-house based on Geometrical Optics (GO) and Geometrical Theory of Diffraction (GTD). The rays considered in GO are direct, reflected and refracted rays interacting within the elements of the scenario under analysis. To complement the GO theory, the diffracted rays are introduced with the GTD and its uniform extension, the Uniform GTD (UTD) [50–52]. The purpose of these rays is to remove the field discontinuities and to introduce proper field corrections, especially in the zero-field regions predicted by GO. The basic procedure of the ray launching algorithm [50–52] is, first, to launch a ray from the transmitting antenna (noted as Tx). Then,

the ray is traced to see if it hits any object or is received by the receiving antenna. When the ray impacts with an obstacle, reflection, transmission and diffraction will occur, depending on the geometry and the electric properties of the object. Once all possible paths have been identified, high-frequency electromagnetic techniques, such as UTD [50] are applied to the rays to compute the amplitude, phase, delay, and polarization of each ray. The implemented algorithm takes into account Fresnel equations, discretized within the cuboids present in the simulation volume, in which the reflection coefficient $R^{\perp}$ and transmission coefficient $T^{\perp}$ are calculated by

$$T^{\perp} = \frac{E_t^{\perp}}{E_i^{\perp}} = \frac{2\eta_2 \cos(\Psi_i)}{\eta_2 \cos(\Psi_i) + \eta_1 \cos(\Psi_t)} \tag{1}$$

$$R^{\perp} = \frac{E_r^{\perp}}{E_i^{\perp}} = \frac{\eta_2 \cos(\Psi_i) - \eta_1 \cos(\Psi_t)}{\eta_2 \cos(\Psi_i) + \eta_1 \cos(\Psi_t)} \tag{2}$$

where $\eta_1 = 120\pi/\sqrt{\varepsilon_{r1}}$, $\eta_2 = 120\pi/\sqrt{\varepsilon_{r2}}$ and Ψ_i, Ψ_r and Ψ_t are the incident, reflected and transmitted angles respectively. Several transmitters can be placed within the scenario, in which power is modeled as a finite number of rays launched within a solid angle. Parameters such as frequency of operation, radiation patterns of the antennas, number of multipath reflections, separation angle between rays, and cuboids dimension are introduced. The material properties for all the elements within the scenario are considered, given the dielectric constant and the loss tangent at the frequency range of operation of the system under analysis.

Figure 1 shows the principle of ray launching method. The transmitter antenna launches rays in different directions following
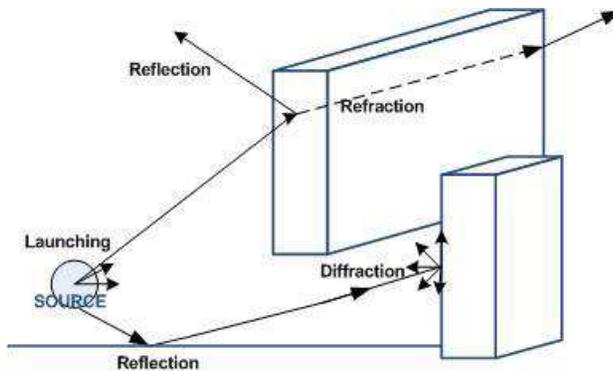

Figure 1. Principle of ray launching method.

the radiation pattern of the antenna. The reflection and refraction coefficients are calculated using the well-known Fresnel's equations and the diffraction coefficients by the Uniform Theory of Diffraction (UTD) [50]. The commitment between accuracy and computational time is acquired with the number of launching rays and the cuboids size of the considered scenario. The considered scenario is an indoor room of dimensions $6.5\,\text{m} \times 5.5\,\text{m} \times 2.5\,\text{m}$ with different objects and with a human body model in the center. Objects are defined as different hexahedrons in the algorithm. By this basic geometric shape it is highly easy to form another objects much more complex, such as tables, chairs and shelves, and placing them into the room. In a generic room, walls can be formed by windows, doors, frames, etc. So, to characterize the walls of a room, each discontinuity on the wall must be characterized. This will define each part of the wall like an object by its central position $(x_0,\ y_0,\ z_0)$, the width in each dimension $(\Delta x,\ \Delta y,\ \Delta z)$ and the material that is made. A schematic view of the simulated scenario is depicted in Figure 2, with some typical objects of an office
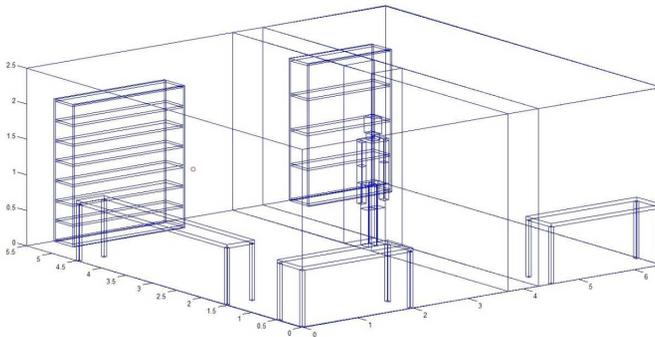
**Figure 2.** Schematic view of the considered scenario.

Table 1. Simulation parameters employed by the RL code developed at UPNA.

PARAMETERS IN THE RAY LAUNCHING SIMULATION	
Frequency	2 GHz
	2.4 GHz
Vertical plane angle resolution $\Delta\theta$	1°
Horizontal plane angle resolution $\Delta\varphi$	1°
Reflections	7
Transmitter Power	4.5 dBm

room, specifically three tables and two shelves.The transmitter antenna has been placed at the point (0.75 m, 3 m, 1.5 m). Simulations have been done for two different working frequencies, 2 GHz and 2.4 GHz. Table 1 shows the parameters used in simulation.

In the analyzed scenario, two different areas have been considered to perform a more precise analysis of the influence of electromagnetic waves in the human body, to optimize computational cost without compromising accuracy.   Therefore, a high resolution and low resolution areas have been defined. The high resolution area (Figure 3) is located at the center of the scenario (Figure 2), with a reduced size 0.55 m × 0.55 m × 2.5 m, in which the model of the human body is located.

Resolution is defined in the 3D Ray launching algorithm by the size of the cuboids in which the room is divided to estimate the power level in each of them. In this way, the resolution of the small zone in which the human body has been introduced employs cuboids of size 0.03 m × 0.03 m × 0.2 m. As far as the human body model is concerned, it has been performed with the greatest detail as possible, taking into
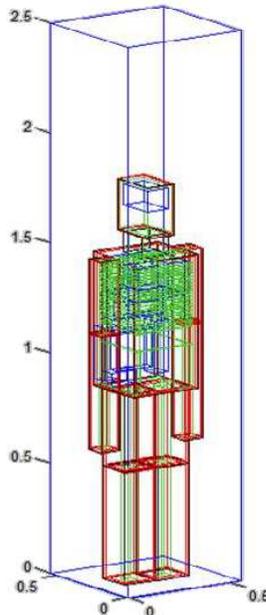
Figure 3. Detail of the high resolution zone, which the different organs that are embedded in the human body model.

account parts such as bones, internal organs, muscles, blood and skin, all with their respective values of dielectric constant and conductivity parameterized to the given frequency range, as given by [53, 54]. Table 2 shows the materials taken into account for simulation. The human body model has been parameterized in such a way that body proportions (i.e., relative dimensions between head, limbs and torso) are maintained for any given height of the person that is needed to be modeled.

To reduce computational cost, it is possible to consider less resolution in the design of the human body model. In this way only skin and bones could be considered, adding organs gradually up to four different types of human body models. In this work, the highest resolution for the human body has been considered. The behavior of such materials is strongly dispersive, as seen in Figures 4 and 5, by parametric calculation of the materials parameters which is automatically performed by the in house code that has been developed for this purpose. Therefore, a dynamic variation of the material properties to take into account the estimation of interaction of electromagnetic waves with different organs is considered in the overall simulation result.

The results of the received power correspond to the high resolution area, which is depicted with the human body in Figure 2. Figures 6 and 7 show horizontal planes of received power in two different heights ($Z = 1$ m and $Z = 1.6$ m) for operating frequencies of a wireless source of 2 GHz and 2.4 GHz, respectively. Figures 8 and 9 depict the vertical sections of the zone of high resolution keeping constant the value of X in 0.3 m.

Table 2. Dielectric constant and conductivity for different parts of the body at different frequencies.

	ε_r		Conductivity [S/m]	
Frequency	**2 GHz**	**2.4 GHz**	**2 GHz**	**2.4 GHz**
Blood	60.50	60.12	18.01	17.01
Bone	20.86	20.63	4.75	4.83
Heart	57.08	56.43	15.75	15.07
Kidney	55.03	54.27	17.45	16.47
Liver	44.91	44.42	11.46	11.16
Muscle	54.44	54.16	11.69	11,29
Dry skin	38,53	38,03	11,41	10.82
Small intestine	56.66	56.03	24.04	21.94

It can be seen that the wave impinges with more power on the left side of the human body model, due to the fact that the source is located in this direction and direct wave has more power than the reflected waves. The morphology of the human body also influences the way in which power is distributed through space. There is an important difference between one meter height, where is the waist of the body and the height of 1.6 m where the wave hits the head, given by the consideration of different material parameters embedded in the model. It can also be seen that the election of the frequency plays a key role in the characterization of the radio propagation channel, with a higher estimation of received power for lower frequencies.
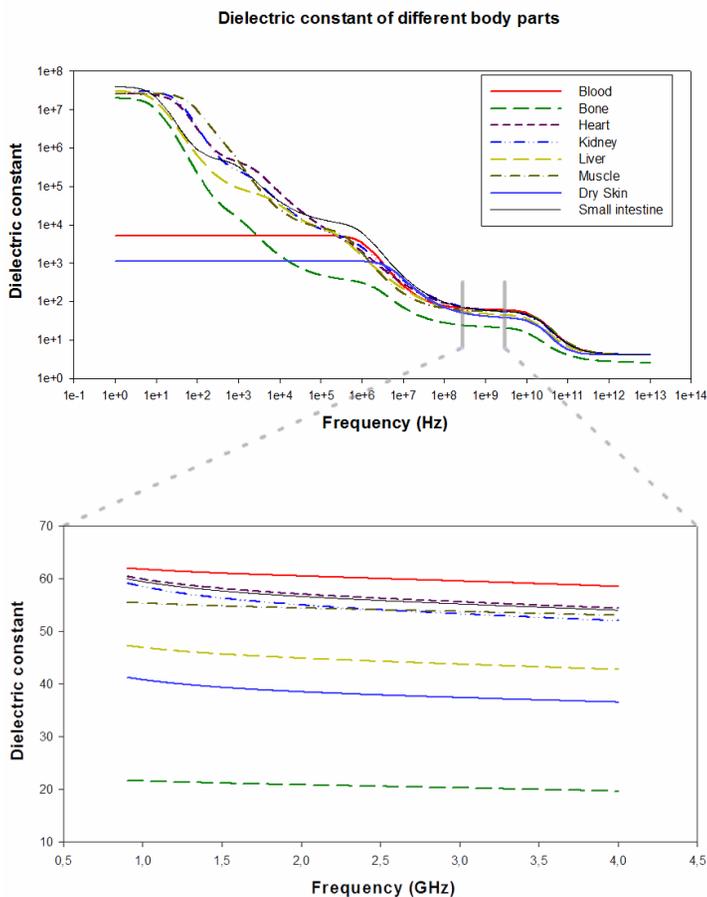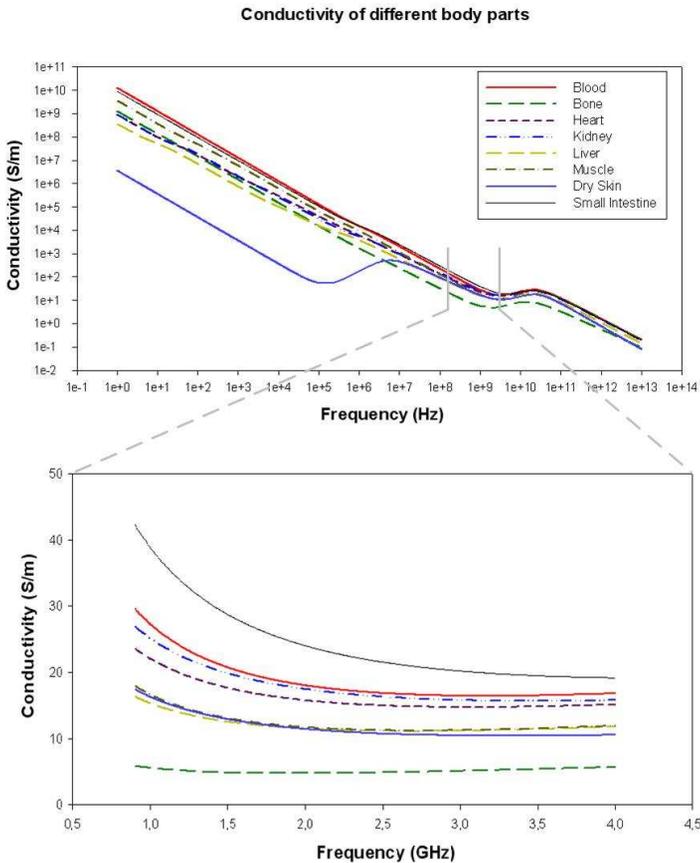

Figure 4. Estimation obtained of the dielectric constant shift versus frequency for different parts of the human body model developed.

In order to analyze more thoroughly the data, Figure 10 represents the estimation of received power for the high resolution zone with the Y axis value of 0.275 m and Z dimension ranging for different heights, between 0.4 m to 2 m.

As expected, the estimated received power decreases with higher frequencies. Such behavior is dictated by the radio propagation characteristic and the frequency response of dispersive materials presenting in the human body model. It is also observed strong degree of variability in the received power. This is due to the fact that the fundamental propagation phenomena in an indoor environment is multipath propagation, which is characterized by the temporal

Figure 5. Estimation obtained of the Conductivity shift versus frequency for different parts of the human body model developed.
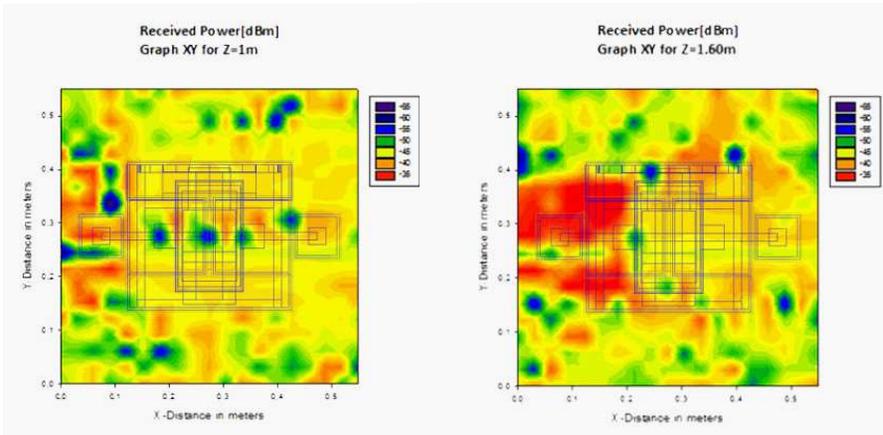
Figure 6. Estimation of Received power for two different heights in the *XY* plane with the human body model overhead (2 GHz).
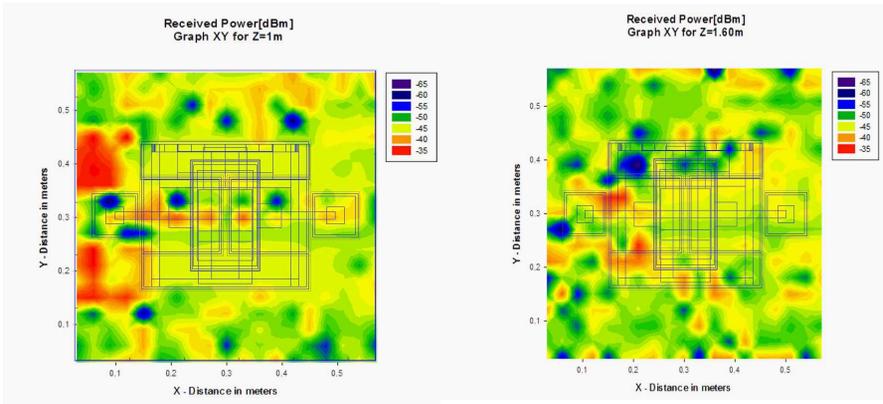
Figure 7. Estimation of Received power for two different heights in the *XY* plane with the human body model overhead (2.4 GHz).

dispersion of the signal and the frequency dispersion due to temporal variations of the received amplitude.

3. MEASUREMENT RESULTS

To validate previous predictions, measurements in a real scenario with a real person have been performed. For this purpose, the ground floor of the research center Jerónimo de Ayanz of the Public University of Navarre has served as the set up for the experiments, whose geometry

is shown in Figure 11. All materials within the scenario have been taking into account for the simulation, like concrete for the walls and columns, glass for the windows, metal for the elevator and wood for the doors, considering their dielectric constant and conductivity for the given frequency of operation. The scenario dimensions are $19.6\,\text{m} \times 13.6\,\text{m} \times 3.8\,\text{m}$.

The wideband measurements were performed with 100 MHz bandwidth at 2.4 GHz frequency. The transceivers are from Texas Instruments, specifically the CC2530 that is a true system-on-chip (SoC) solution for IEEE 802.15.4 ZigBee. The radiation pattern of the transceivers is omnidirectional with linear polarization and 0.82 dBi gain. Measurements have been made with the transmitter fixed at the point XY (8.51 m, 11.29 m) with a 0.60 m height. The transmitter power is 4.5 dBm.

In order to perform the measurements, three different positions of
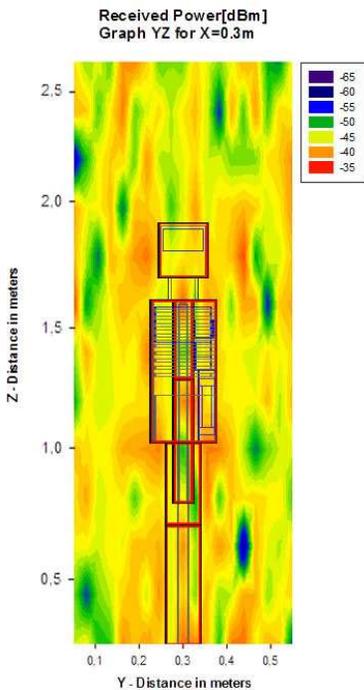
Figure 8. Estimation of received power for the plane YZ (2 GHz).
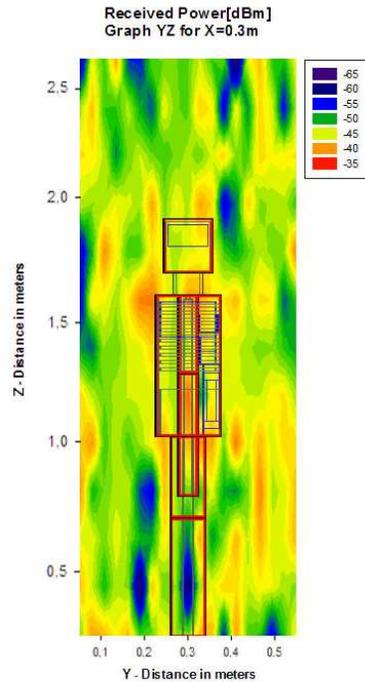
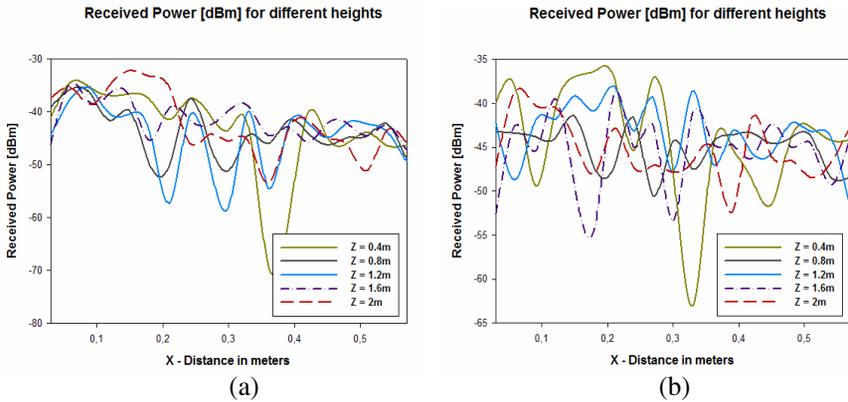**Figure 9.** Estimation of received power for the plane YZ (2.4 GHz).

Figure 10. Estimation of received power for different heights within the simulation scenario. (a) $f = 2\,\text{GHz}$, (b) $f = 2.4\,\text{GHz}$.
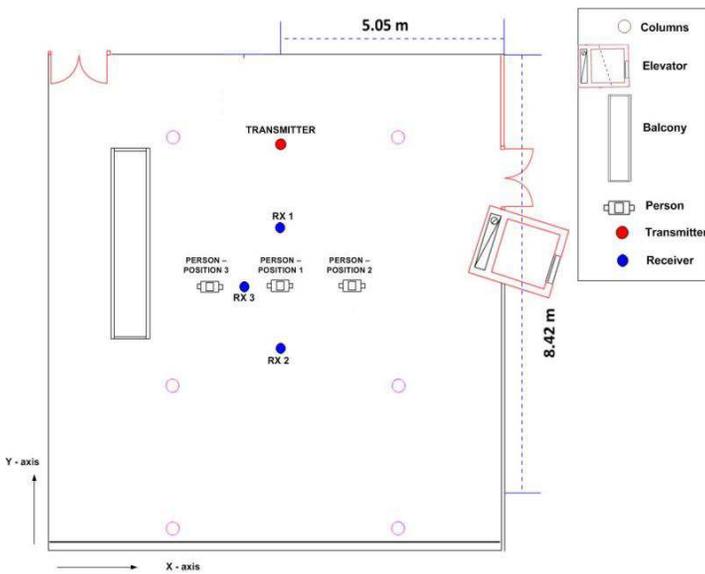

Figure 11. Scenario considered for the measurements.

the person have been considered, which are depicted in Figure 11 and correspond to the points XY $(6.07\,\text{m}, 7.69\,\text{m})$, $(8.61\,\text{m}, 7.69\,\text{m})$ and $(11.23\,\text{m}, 7.69\,\text{m})$. For each position of the person in the considered scenario, nine measurements have been performed. The first three measurements correspond to the three points of reception shown in Figure 11. The election of these points is designed to assess the
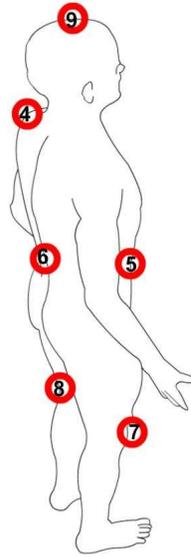
Figure 12. Measurement points in the real person.

influence of the human body in different points of the environment, taking into account free space between transmitter and receiver for RX 1 and the presence of a person between them for RX 2. The remaining six measurement points agree with the points represented in Figure 12 for different parts of the human body. In the process of measures, the person was always looking ahead to the transmitter. To evaluate the influence of the different organs which make up the human body in the environment, different points of the front of the human body have been chosen, specifically, the abdomen and the right knee and the shoulder and back knee for the rear of the body.

A portable spectrum analyzer from Agilent (N9912 Field Fox) has been used for the experiments. The measurement time at each point was 60 seconds, and the power value represented by each point was the higher peak of power shown by the spectrum analyzer for the considered bandwidth (*MaxHold* function in the spectrum analyzer of Agilent).

Figure 13 shows the comparison between simulation and measurements, exhibiting good agreement with a mean error around 2 dB for all cases. The differences are mainly due to approximations made in simulation. It is also important to consider the fast fading, which is a relevant effect in indoor environments that occur due to the multipath components which are very significant. It is observed that
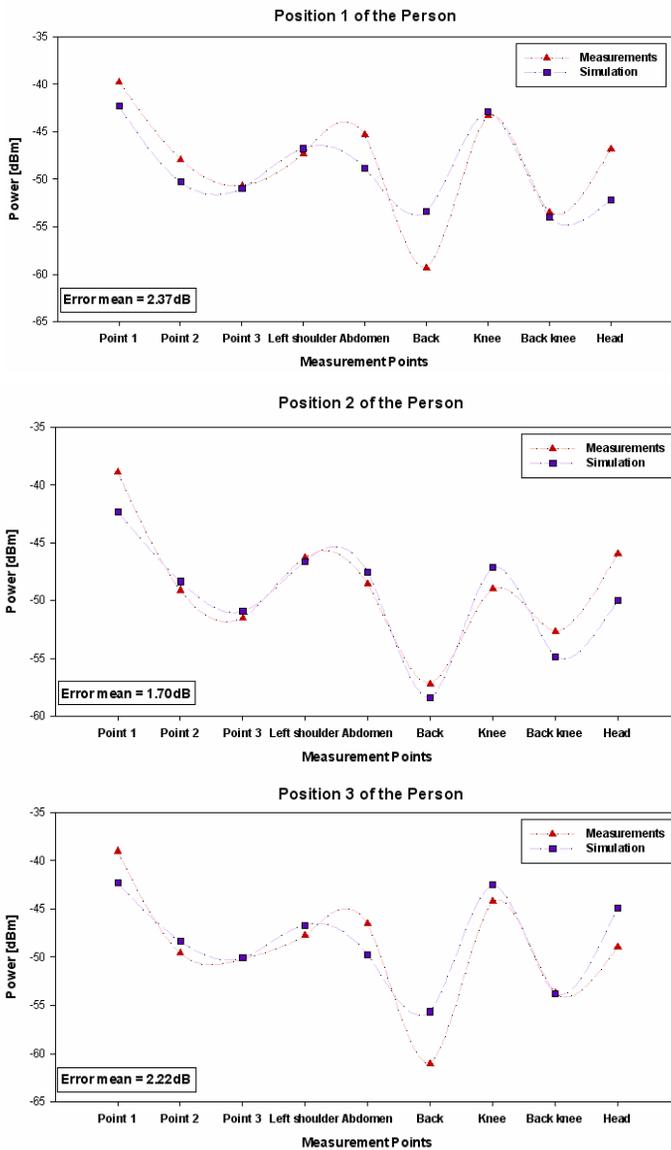
Figure 13. Comparison simulation versus measurements for different positions of the person.

there are no significant differences between the three positions of the person in terms of power levels received at each position. Nevertheless, for the three cases, received power level is lower for the position 2 of

the receiver (RX 2 of Figure 11) due to the presence of the human body between the transmitter and the receiver. It is also shown that the influence of the person for point 3 (RX 3 of Figure 11) is also considerable, comparing with the position 1 (RX 1 of Figure 11) which is facing the transmitter. It is also perceived that the received power levels for the measurement points of the front part of the body, specifically the abdomen and the knee (Point 5 and 7 of Figure 12), are higher values than the rear part, back and back knee (Point 6 and 8 of Figure 12). This is due to the human body penetration losses which are present in the radio electric path. It is observed that these losses are bigger in the abdomen part of the body than in the knee, due to the higher volume of mass as well as to the higher volume of liquid content in the first case.

4. CONCLUSIONS

In this work, the influence of a human body in dosimetry evaluations has been analyzed. A simplified human body model, including the dispersive nature of material parameters of internal organs has been implemented. The use of deterministic 3D ray launching algorithm implemented in-house combined with the human body model allows the performance of dosimetric estimations for indoor scenarios considering the electromagnetic sources and the presence of several persons in the same scenario. Simulations as well as measurement results have been presented, showing good agreement between them. This simulation approximation can be used in order to assess the influence of electromagnetic exposure due to the combined operation of several wireless systems in indoor heterogeneous scenarios, with results given for the full extent of such simulation scenario.

ACKNOWLEDGMENT

REFERENCES

1. World Health Organizations, "Framework for developing health-based EMF standards," EMF Project, http://www.who.int/peh-emf/standards/framework/en/index.html.
2. http://www.icnirp.org/documents/emfgdl.pdf.

3. *Biologic Effects and Health Hazards of Microwave Radiation*, Polish Medical Publication, Warsaw, 1974.

4. Wang, J. and O. Fujiwara, "Uncertainty evaluation of dosimetry due to plastic holder for restraining small animal in Vivo near field exposure setup," *IEEE Trans. on EM Comp.*, Vol. 46, No. 2, May 2004.

5. Wang, J. and O. Fujiwara, "Dosimetricanalysis of a small animal locally exposed to near fields by electrically short antennas," *International Symposium Electromagnetic Compatibility*, 1999.

6. Zhadobov, M., R. Sauleau, Y. L. Dréam, S. I. Alekseev, and M. C. Ziskin, "Numerical and experimental millimeter-wave dosimetry for in vitro experiments," *IEEE Trans. on Microwave Theory and Techniques*, Vol. 56, No. 12, Dec. 2008.

7. Tinniswood, A. D. and C. M. Furse, "Computations of SAR distributionsfor two anatomically-basedmodels of the human head using CAD files of commercial telephonesand the parallelized FDTD code," *1997 Digest IEEE Antennas and Propagation Society International Symposium*, 1997.

8. Nagaoka, T. and S. Watanabe, "GPU-based 3D-FDTD computation for electromagnetic field dosimetry," *IEEE Africon 2011 — The Falls Resort and Conference Centre*, 13–15, Livingstone, Zambia, Sep. 2011.

9. Tailor, H. C., J. W. Hand, and R. W. Lau, "FDTD modelling for microwave dosimetry and thermcigraphy," *IEEE Colloquium on Application of Microwaves in Medicine*, Feb. 28, 2005.

10. Angulo, L. D., S. G. Garcia, M. F. Pantoja, C. C. Sanchez, and R. G. Martín, "Improving the SAR distribution in petri-dish cell cultures," *Journal of Electromagnetic Waves and Applications*, Vol. 24, Nos. 5–6, 815–826, 2010.

11. Sato, R., H. Sato, and H. Shirai, "A SBR algorithm for simple indoor propagation estimation," Faculty of Education and Human Sciences, Niigata University, Faculty of Science and Engineering, Chuo University, Tokyo, Japan, 2005.

12. Shirai, H., R. Sato, and K. Otoi, "Electromagnetic wave propagation estimation by 3-D SBR method," *International Conference on Electromagnetics in Advanced Applications, ICEAA*, Sep. 2007.

13. Ling, F., Q. Sheng, and J. M. Jin, "Hybrid MoM/SBR and FEM/SBR methods for scattering by large bodies with inhomogeneous protrusions," *1997 Digest IEEE Antennas and Propagation Society International Symposium*, Jul. 13–18, 1997.

14. Durney, C. H., M. F. Iskander, H. Massoudi, and C. C. Johnson,

"An empirical formula for broad-band SAR calculations of prolate spheroidal models of humans and animal," *IEEE Trans. on Microwave Theory and Techniques*, Vol. 27, No. 8, Aug. 1979.

15. Poljak, K. and N. Kovac, "The electromagnetic-thermal analysis of human exposure to radio base station antennas," *17 International Conference on Applied Electromagnetics and Communications*, Dubrovnik, Croatia, Oct. 1–3, 2003.

16. Ruan, F., T. Duglosz, D. Shi, and Y. Gao, "Cylinder model of human body impedance based on proximity effect," *3rd IEEE International Symposium on Microwave, Antenna, Propagation and EMC Technologies for Wireless Communications*, Oct. 27–29, 2009.

17. Ghaddar, M., L. Talbi, and T. A. Denidni, "Human body modelling for prediction of effect of people on indoor propagation channel," *Electronics Letters*, Vol. 40, No. 25, Dec. 9, 2004.

18. Uzunoglu, N. K. and E. A. Angelikas, "Field distributions in a three-layer prolate spheroidal human body model for a loop antenna irradiation," *IEEE Trans. on Antennas and Propagation*, Vol. 35, No. 10, Oct. 1987.

19. Reivomen, S., T. Keikko, J. Isokorpi, and L. Korpinen, "Internal currents in a human body with spheroidal model in 400 kv switching substation," *IEEE Symposium on High Voltage Engineering*, No. 461, Aug. 21–22, 1999.

20. Durney, C. H., C. C. Johnson, and H. Massoudi, "Long-wavelength analysis of plane wave irradiation of a prolate spheroid model of man," *IEEE Trans. on Microwave Theory and Techniques*, Feb. 1975.

21. Canseven, A. G. and N. Seyhan, "Ellipsoid models for human and guinea pigs exposed to magnetic fields," *IEEE International Symposium on Electromagnetic Compatibility*, May 11–16, 2003.

22. Özen, S., S. Çömlekçi, and O. Çerezci', "An evaluation for coupling of human to magnetic fields in human ellipsoidal models with frequency up to 100 kHz," *Proceedings of the 23rd Annual IEEE EMBS International Conference*, 25–28, Oct. 2001.

23. Massoudi, H., C. H. Durney, and C. C. Johson, "Long-wavelength electromagnetic absorption in ellipsoidal model man and animals," *IEEE Trans. on Microwave Theory and Techniques*, Vol. 25, No. 1, Jan. 1977.

24. Surda, J., E. Cocherova, and O. Ondracek, "Tissue parameters influence on the microwave energy absorption in biological objects," *14th Conference on Microwave Techniques*, 1–4, 2008.

25. Nagaoka, T. and S. Watanabe, "Development of anatomically realistic whole-body models of children and their use in electromagnetic dosimetry," *Cairo International Biomedical Engineering Conference*, 2008.

26. Dawson, T. W. and M. A. Stuchly, "High-resolution organ dosimetry for human exposure to low-frequency magnetic fields," *IEEE Transactions on Magnetics*, Vol. 34, No. 3, May 1998.

27. Nagaoka, T. and S. Watanabe, "Japanese voxel-based computational models and their applications for electromagnetic dosimetry," *XXXth URSI General Assembly and Scientific Symposium*, 2011.

28. Chuang, H. R. and W. T. Chen, "Computer simulation of the human-body effects on a circular-loop-wire antenna for radio-pager communications at 152, 280, and 400 MHz," *IEEE Trans. Veh. Tech.*, Vol. 46, No. 3, Aug. 1997.

29. Fujii, K., M. Takahashi, K. Ito, and N. Inagaki, "Study on the electric field distributions around whole body model with a wearable device using the human body as a transmission channel," *First European Conference on Antennas and Propagation*, 2006.

30. Chuang, H. R., "Numerical computation of fat layer effects on microwave near-field radiation to the abdomen of a full-scale human body model," *IEEE Trans. on Microwave Theory and Techniques*, Vol. 45, No. 1, Jan. 1997.

31. Lazzi, G. and O. P. Gandhi, "Realistically tilted and truncated anatomically based models of the human head for dosimetry of mobile telephones," *IEEE Transactions on Electromagnetic Compatibility*, Vol. 39, No. 1, Feb. 1997.

32. Fahs, H., A. Hadjem, S. Lanteri, J. Wiart, and M. F. Wong, "Calculation of the SAR induced in head tissues using a high-order DGTD method and triangulated geometrical models," *IEEE Trans. on Antennas and Propagation*, Vol. 59, No. 12, Dec. 2011.

33. Iskander, M. F., H. Massoudi, C. H. Durney, and S. J. Allen, "Measurements of the RF power absorption in spheroidal human and animal phantoms exposed to the near field of a dipole source," *IEEE Transactions on Biomedical Engineering*, Vol. 28, No. 3, Mar. 1981.

34. Commens, M. and L. Williams, "Strategies for effective use of EM simulation for SAR," *International Symposium on Electromagnetic Compatibility*, 2004.

35. Seidel, S. Y. and T. S. Rappaport, "Site-specific propagation prediction for wireless in building personal communication system design," *IEEE Trans. Veh. Tech.*, Vol. 43, 879–891, Nov. 1994.

36. Durney, C. H., "Electromagnetic dosimetry for models of humans and animals: A review of theoretical and numerical techniques," *Proceedings of the IEEE*, Vol. 68, No. 1, Jan. 1980.

37. Bernardi, P., M. Cavagnoro, S. Pisa, and E. Piuzzi, "Specific absorption rate and temperatura increases in the head of celular-phone user," *IEEE Trans. on Microwave Theory and Techniques*, Vol. 48, No. 7, 1118–1126, Jul. 2000.

38. Gritsenko, N. V., A. Y. Bijamov, A. Razmadze, L. S. Shoshi-ashvili, and R. S. Zaridze, "Simulation of the thermal effects in the human head due to the RF exposure," *Proceedings of the 9th International Seminar/Workshop on Direct and Inverse Problems of Electromagnetic and Acoustic Wave Theory, 2004, DIPED 2004*, 87–89, Oct. 2004.

39. Salford, L. G., A. Brun, J. Eberhardt, L. Malmgren, and B. Persson, "Electromagnetic field-induced permeability of the blood-brain barrier shown by immunohistochemical methods," *Interaction Mechanism of Low-Level Electromagnetic Fields in Living Systems*, B. Nordén and C. Ramel, eds., 251–258, Oxford University Press, Oxford, 1992.

40. Salford, L. G., A. Brun, K. Sturesson, J. L. Eberhardt, and B. R. R. Persson, "Permeability of the blood-brain-barrier induced by 915 MHz electromagnetic-radiation, continuous wave and modulated at 8, 16, 50 and 200 Hz," *Microscopy Research and Technique*, Vol. 27, No. 6, 535–542, 1994.

41. Lee, S.-H., "A photon modeling method for the characterization of indoor optical wireless communication," *Progress In Electromagnetics Research*, Vol. 92, 121–136, 2009.

42. Lee, D. J. Y. and W. C. Y. Lee, "Propagation prediction in and through buildings," *IEEE Trans. Veh. Tech.*, Vol. 49, No. 5, 1529–1533, 2000.

43. Tan, S. Y. and H. S. Tan, "A microcellular communications propagation model based on the uniform theory of diffraction and multiple image theory," *IEEE Trans. on Antennas and Propagation*, Vol. 44, No. 10, 1317–1326, 1996.

44. Kanatas, A. G., I. D. Kountouris, G. B. Kostaras, and P. Constantinou, "A UTD propagation model in urban microcellular environments," *IEEE Trans. Veh. Tech.*, Vol. 46, No. 1, 185–193, 1997.

45. Dimitriou, A. G. and G. D. Sergiadis, "Architectural features and urban propagation," *IEEE Trans. on Antennas and Propagation*, Vol. 54, No. 3, 774–784, 2006.

46. Franceschetti, M., J. Bruck, and L. J. Schulman, "A random

walk model of wave propagation," *IEEE Trans. on Antennas and Propagation*, Vol. 52, No. 5, 1304–1317, 2004.

47. Blas Prieto, J., R. M. Lorenzo Toledo, P. Fernández Reguero, E. J. Abril, A. Bahillo Martínez, S. Mazuelas Franco, and D. Bullido, "A new metric to analyze propagation models," *Progress In Electromagnetics Research*, Vol. 91, 101–121, 2009.

48. Schuster, J. W. and R. J. Luebbers, "Comparison of GTD and FDTD predictions for UHF radio wave propagation in a simple outdoor urban environment," *IEEE Antennas and Propagation Society International Symposium*, Vol. 3, 2022–2025, 1997.

49. Iskander, M. F. and Z. Yun, "Propagation prediction models for wireless communications systems," *IEEE Trans. on Microwave Theory and Techniques*, Vol. 50, 662–673, 2002.

50. Kouyoumjian, R. G. and P. H. Pathak, "A uniform theory of diffraction for an edge in a perfectly conducting surface," *Proceedings of the IEEE*, Vol. 62, No. 4, 1448–1462, 1974.

51. Seidel, S. Y. and T. S. Rappaport, "Site-specific propagation prediction for wireless in-building personal communication system design," *IEEE Trans. Veh. Tech.*, Vol. 43, No. 4, 879–891, 1994.

52. Luebbers, R. J., "A heuristic UTD slope diffraction coefficient for rough lossy wedges," *IEEE Trans. on Antennas and Propagation*, Vol. 36, No. 2, Feb. 1989.

53. Gabriel, C., "Compilation of the dielectric properties of body tissues at RF and microwave frequencies," Tech. Rep. AL/OE-TR-1996–0037, Brooks Air Force, Brooks AFB, TX, 1996.

54. Sánchez-Hernández, D. A., *High Frequency Electromagnetic Dosimetry*, Artech House, Inc., 2009.